Journal of Solid State Chemistry **157,** 76–85 (2001)
doi:10.1006/jssc.2000.9041, available online at http://www.idealibrary.com on IDEAL®

Synthesis, Structure, and Physical Properties of Cobalt Perovskites: $Sr_3CoSb_2O_9$ and $Sr_2CoSbO_{6-\delta}$

Vicent Primo-Martín and Martin Jansen[1]

Max-Planck-Institut für Festkörperforschung, Heisenbergst., 1, 70569 Stuttgart, Germany

Received August 2, 2000; in revised form November 1, 2000; accepted December 1, 2000

The perovskites $Sr_3CoSb_2O_9$, Sr_2CoSbO_6, and $Sr_2CoSbO_{5.63}$ have been synthesized in polycrystalline form by solid state reactions from acetate precursors as obtained by freeze-drying. The crystal structure of insulating $Sr_3CoSb_2O_9$ has been refined from X-ray data by the Rietveld method and was found to be orthorhombic (*Immm*) with $a = 5.6411(1)$ Å, $b = 5.6610(1)$ Å, $c = 7.9829(2)$ Å. From the molar susceptibility curves an effective magnetic moment $\mu_{eff} = 5.39\ \mu_B$ and a spin-glass transition at ca. 6 K are deduced. The semiconducting perovskite Sr_2CoSbO_6 was synthesized by applying an elevated O_2 pressure (3 kbar), and Co exclusively in the oxidation state +3 was attained. The Rietveld refinement of this compound has revealed a rhombohedral cell ($R\bar{3}m$) with $a = 5.5992(2)$ Å and $c = 13.6609(2)$ Å and partial order (77%) of the *B* cations. An effective magnetic moment per formula unit of $\mu_{eff} = 3.83\ \mu_B$ and a spin-glass transition at ca. 47 K were observed. A semiconducting and oxygen-deficient perovskite, $Sr_2CoSbO_{5.63}$, was obtained by annealing Sr_2CoSbO_6 at 950°C in Ar. The Rietveld refinement proved it to be a double-cubic perovskite ($Fm\bar{3}m$) with $a = 7.9658(1)$ Å, and a higher order of Co and Sb at the *B* sites (84%) was found, due to the formation of Co^{2+}. From the magnetic susceptibility data an effective moment of 4.85 μ_B and a spin-glass transition at ca.17 K were deduced.

Key Words: **Cobalt perovskites; Co^{+3} high spin; spin-glass.**

INTRODUCTION

Perovskite oxides of the transition elements have been studied extensively since they present interesting and frequently unexpected magnetic and transport properties. Famous examples are the superconducting mixed-valent copper oxides and the mixed-valent manganese perovskites exhibiting giant magnetoresistance (1). In either case the special physical properties are strongly related to charge-ordering phenomena.

There exists a great variety of cobalt oxide perovskites showing a wide range of properties, e.g., antiferromagnetism, ferromagnetism (2), spin-glass behavior (3), or magnetoresistance (4), depending on the respective compositions. In $ACoO_3$-type perovskites, lanthanum and alkaline-earth elements are usually employed as *A* cations (5) and, among others, Fe and Ru have been used as substitutes for cobalt (6).

The goal of our work presented here has been to prepare and characterize perovskites $SrBO_3$ containing cobalt and antimony in different ratios as *B* cations in order to provoke charge order/disorder phenomena. Cobalt is well known to exhibit a range of different valence states (different oxidation numbers plus high- and low-spin configurations), and Sb is able to adopt two different oxidation states (III and V) and thus can exhibit mixed valency as well. In cases like $Sr_3CoSb_2O_9$ an interesting competition could arise between the two most probable charge distributions, $Co^{+2}(Sb^{5+})_2$ and $Co^{3+}Sb^{4+}Sb^{5+}$, since cobalt, in the environment given, would prefer the valence state +3 while antimony will refuse the state +4. One out of a number of solutions for this situation of frustration could be delocalization of the excess electron yielding metallic behavior. A crucial issue in this context is to control, or at least to determine, the oxygen deficiency. Therefore the syntheses have been performed under defined atmospheres (argon, air, and high O_2 pressure) to tune the oxygen content and thus the oxidation states of the Co and Sb ions.

Blasse studied the structure (7) and magnetic properties (8) of two phases of the title system, $Sr_3CoSb_2O_9$ and Sr_2CoSbO_6, and reported them to be "practically" cubic. In addition, for the latter phase Blasse claimed to have found the first oxide with Co^{3+} being completely in the high-spin ($S = 2$) state (8), due to the high value found (5.2 μ_B) for the effective magnetic moment, from fitting the experimental data to the Curie–Weiss law. It was also considered by Demazeau *et al.* (9) as the definitive Co^{3+} oxide (in octahedral coordination) in high-spin state to compare with some other perovskite-type oxides like $RCoO_3$ (R = La, Y, Gd, etc.). $LaCoO_3$, which also has Co in +3 oxidation state, crystallizes in a rhombohedral perovskite structure, and has been studied thoroughly by Goodenough (10) with

[1] To whom correspondence should be addressed. Fax: 49 711 689 1502. E-mail: martin@jansen.mpituttgart.mpg.de.

0022-4596/01 $35.00

emphasis put on spin transitions that occur at varying temperatures. Recently a number of reports (11) have been published that help definitively establish a consensus upon the spin transitions that occur in $LaCoO_3$: the first transition at ca. 100 K is suggested to lead from LS (low spin) to IS (intermediate spin) state rather than from LS to HS (high spin) state as argued by Señarís and Goodenough (10a), and the second one around 500 K is attributed to the population of the HS from the IS state, leading to a mixture of IS and HS states. Summarizing, with increasing temperature, the sequence LS → IS → HS appears to be likely in the rhombohedral perovskite phase $LaCoO_3$. Another example is depicted by the perovskite Ba_2CoNbO_6 (12), which has been described as cubic with a completely disordered arrangement of the *B* cations ($Pm\bar{3}m$), and the author has stated that it shows a spin-glass transition originated by the magnetic frustration due to the coexistence of high- and intermediate-spin states of the Co^{3+} ions, but further structural proofs of the stabilization of Co^{3+} in the IS state would be necessary. An example of Co^{3+} in IS state is $TlSr_2CoO_5$ (13), which has a perovskite related structure, and Co^{3+} ions are stabilized in *IS* state by elongated deformation of the CoO_6 octahedra.

Here we report on a reinvestigation of strontium cobalt antimonate perovskites, which lead to significant discrepancies in the previous work mentioned in particular with respect to the possible existence of Co^{3+} in a pure high-spin state in an octahedral environment of oxygen.

EXPERIMENTAL

All samples have been synthesized via solid state reactions using acetate precursors obtained by freeze-drying (14). The solutions used for freeze-drying were obtained by dissolving the necessary amounts of Sb_2O_3 (Merck, 99.95%) in glacial acetic acid (~ 175 ml/g Sb_2O_3) while refluxing; $Sr(Ac)_2 \cdot \frac{1}{2}H_2O$ (Fluka, 99.99%) was subsequently added to the former transparent solution along with a few milliliters of H_2O; and finally $Co(Ac)_2 \cdot 4H_2O$ (Alfa, 99.99%) was added and dissolved upon stirring. The final pink acetic solutions were droplet-frozen into liquid nitrogen and afterward freeze-dried at a pressure of 0.07 mbar using a commercial freeze-dryer (Chris, Beta 2–16). Very fine pink pale powders were obtained by this procedure. The perovskite oxides were synthesized by pyrolysis of these freeze-dried acetate precursors in three steps with intermediate regrinding: 600°C (~ 30 min), 1100°C (2 h), and 1300–1350°C (5–10 h) in air. ZrO_2 yttria-stabilized crucibles were used to minimize the undesired reaction of Co with crucibles. The Sb-rich perovskite $Sr_3CoSb_2O_9$ was oxygen stoichiometric as in air or oxygen synthesized and even after Ar annealing. The sample with the ratio Co:Sb 1:1 was black and slightly oxygen deficient as in air-synthesized $Sr_2CoSbO_{5.95(1)}$. To obtain a fully oxidized phase, the resulting powders from the synthesis in air were sealed in gold capsules and put down in home made autoclaves at 350°–400°C for 12 h applying an O_2 pressure of ca. 3000 bars. Annealing $Sr_2CoSbO_{5.95(1)}$ in Ar at 950°C for 15 h produced a higher oxygen-deficient perovskite with formula $Sr_2CoSbO_{5.63(1)}$. All samples were single phase as checked by X-ray powder diffraction.

All product phases were identified by powder X-ray diffraction using a Stoe Stadi P diffractometer equipped with monochromatic Cu$K\alpha_1$ radiation and a linear position sensitive detector. The samples were filled into a 0.1-mm-diameter capillary (Debye–Scherrer mode). The FullProf v98.02 program (15) was used to refine the crystal structures by the Rietveld method. The refinements were carried out in several space groups, and a pseudo-Voigt shape function was always adequate to obtain good fits. DRXWin and CreaFit v2.2 (16) programs were used as complementary analytical and graphical tools to facilitate the structural refinement.

The initial cationic ratios were confirmed to be maintained in the final oxides by inductively coupled plasma emission spectroscopy (ICP-OES) analysis carried out using an ARL 3580B spectrometer. The analyses of the Co and Sb formal oxidation states and so the oxygen contents were performed by means of standard iodometric titration.

The magnetic susceptibility measurements on powder samples were carried out with a commercial SQUID magnetometer (Quantum Design, MPMS-7.0) applying magnetic fields of 0.1 T and 3 T. All measurements were performed by warming the sample in the applied field after cooling to 2 K in zero field (ZFC, zero field cooling) and by cooling the sample in the measuring field (FC, field cooling). The molar magnetic susceptibilities were corrected for the diamagnetic contributions of each ion (17) except for those of Co^{2+} and Co^{3+} ions, which revealed a temperature-independent paramagnetism (Van Vleck's TIP) (18). This TIP is often roughly the same as the underlying diamagnetic contribution and so it is preferable not to make any correction and assume an approximate cancellation of the two effects (19).

Measurements of the electric resistivity were performed on sintered pellets of ca. 1mm in height using a Hewlett–Packard 3457A multimeter. The resistivity data were obtained by applying the van der Pauw (four-point probe) method.

RESULTS AND DISCUSSION

Two cationic stoichiometries ($x = \frac{1}{3}$ and $x = 0.5$) belonging to the $SrCo_xSb_{1-x}O_{3-\gamma}$ system have been selected for study. The composition with $x = \frac{1}{3}$ produces a full oxygen stoichiometric perovskite, $Sr_3CoSb_2O_9$, with Co in $+2$ oxidation state as either in air or O_2 synthesized or in Ar annealed. It would be very interesting to get an oxygen-deficient perovskite for this cation stoichiometry

because that would mean that part of Sb could be in the $+3$ oxidation state. Initial stoichiometries with $x < \frac{1}{3}$ always yielded $Sr_3CoSb_2O_9$ ($x = \frac{1}{3}$) along with several Sr–Sb–O phases. Perovskite phases with x less than $\frac{1}{3}$ would have matched one of our main goals: mixed valency of Sb cations at the B site. In this respect we were unsuccessful even using high pressure techniques (Belt apparatus) (20). Structure and physical properties of $Sr_2CoSbO_{6-\delta}$ are strongly influenced by oxygen content and therefore three different oxygen stoichiometries have been investigated: $\delta = 0$, 0.05, and 0.37.

Structural Characterization

The $Sr_3CoSb_2O_9$ perovskite was previously described in the literature as an ordered double-perovskite showing a cubic cell with $a = 7.99$ Å (7). However our X-ray diffraction patterns of samples of this compound show considerable splitting of some reflections (Fig. 1), indicating that the crystal symmetry is lower. Significative enough, the doublet featured in Fig. 1 (see inset) comes from the splitting of the (444) reflection as referred to the cubic double-perovskite cell ($Fm\bar{3}m$, $2a_p \times 2a_p \times 2a_p$). This intensity-symmetric splitting of the (444) cubic reflection can only be explained in an orthorhombic unit cell $\sqrt{2}a_p \times \sqrt{2}a_p \times 2a_p$ with indices (044) and (404). The whole pattern can be indexed based on an orthorhombic cell with $a = 5.6411(1)$ Å, $b = 5.6610(1)$ Å, and $c = 7.9829(2)$ Å, which is able to account for this splitting and all the reflections observed in the experimental pattern including the superstructure reflections. The latter are signaling a certain degree of order between the Co and the Sb at the B sites (Fig. 1). The large difference between the X-ray scattering factors of Co and the Sb (26.989 and 50.998 for $\sin\theta/\lambda = 0$, respectively) allows evaluation of the degree of order of the B cations. The refinement of the structure in the orthorhombic space group *Immm* (No. 71) resulted in one of the B sites being almost fully occupied by Sb, while the remaining one contains Co and Sb randomly distributed (ca. $\frac{2}{3}$ Co + $\frac{1}{3}$ Sb). Careful investigation of FWHM of the superlattice reflections, mainly those at low-diffraction angles like (011) and (101), reveals that they are larger than those of the sublattice. This indicates a smaller size of the ordered domains compared to the whole crystal, that is, in this partial structure some degree of short-range order exists rather than full long-range order. Extending the thermal annealing could sharpen these superlattice reflections.

Although the reliability factors are low ($R_{wp} = 5.64$, $R_p = 4.5$, $R_F = 7.23$, $\chi^2 = 1.17$), it should be emphasized that due to the insensitivity of the X-ray powder diffraction data to refine oxygen positions when heavy atoms are present in the structure, the accuracy of the oxygen positions as determined in our refinements should not be overestimated. Table 1 shows the main results of the Rietveld refinement for $Sr_3CoSb_2O_9$. The metric deviations from the ideal cubic

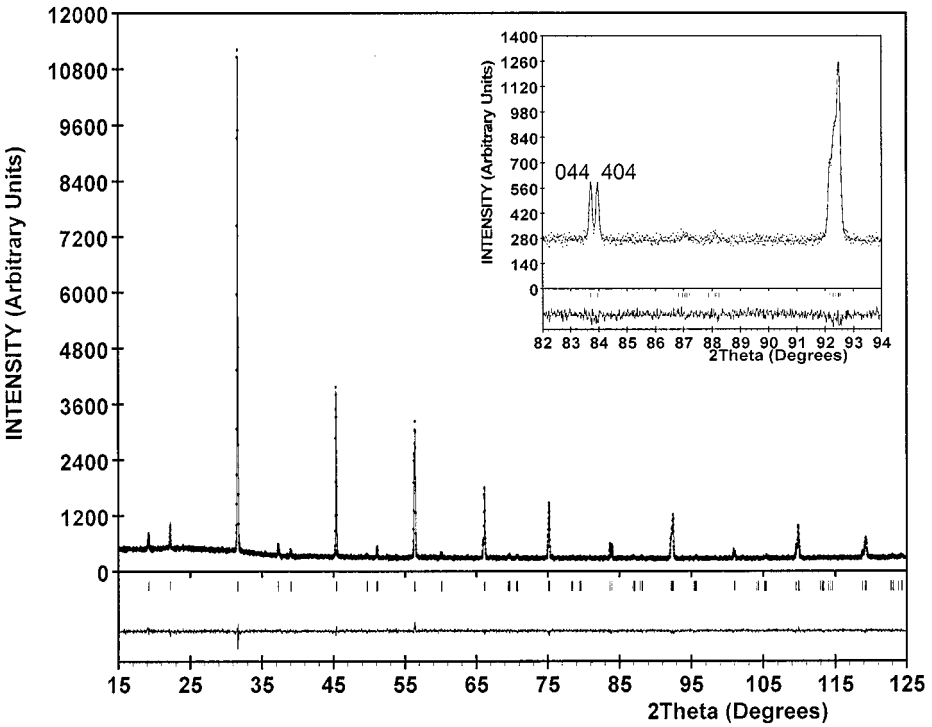

FIG. 1. Rietveld refinement profiles: observed (dots), calculated (solid line), difference (bottom solid line), and bragg reflections (tick marks) for the fit to the Cu$K\alpha_1$ X-ray pattern of the $Sr_3CoSb_2O_9$ perovskite.

TABLE 1
Results of the X-Ray Refinement of $Sr_3CoSb_2O_9$ in the Space Group *Immm* (No. 71)

Atom	Site	x	y	z	B_{iso} (Å^2)	Occupancy
Sr	4j	0.5	0	0.2490(89)	1.43(5)	1
Co(1)	2c	0.5	0.5	0	0.04(5)	0.020(8)
Sb(1)						0.980(8)
Co(2)	2a	0	0	0	0.58(9)	0.644(8)
Sb(2)						0.356(8)
O(1)	8n	0.2572(52)	0.2385(60)	0	2.26(41)	1
O(2)	4i	0	0	0.2499(80)	3.70(88)	1

Note. Lattice parameters (Å): $a = 5.6411(1)$, $b = 5.6610(1)$, $c = 7.9829(2)$. R factors (%): $R_{wp} = 5.64$, $R_p = 4.5$, $R_F = 7.23$, $\chi^2 = 1.17$.

perovskite are rather small ($a = 3.989$, $b = 4.003$, $c = 3.991$),[2] as is also indicated by a Goldschmidt's tolerance factor ($t = 0.94$) close to unity. Since the tolerance factor is less than unity the Sr–O bond is under tension, and the departure from cubic symmetry is mainly due to the cooperative octahedral tilting usually found in the perovskite-type oxides to minimize the tension of the A–O bond. Applying the nomenclature as introduced by Glazer (21), and expanded by Woodward (22), about octahedral tilting in perovskites, this kind of distortion from cubic symmetry could be assigned to the $a^0b^-b^-$ tilt. In case of a uniform occupation of the B site and for this octahedral tilt *Imma* would be the correct space group. But as in the present case some degree of order is accomplished, it is necessary to use a less symmetric space group that allows us to distinguish between B and B' sites. *Immm* is not a maximal nonisomorphic subgroup of *Imma*; however, all of the type I maximal nonisomorphic subgroups of *Imma* have *Immm* as a minimal nonisomorphic supergroup. Therefore *Immm* is the least symmetrical possible orthorhombic space group related to *Imma* that is able to accommodate ordering in the B site. In conclusion *Immm* is a reasonable space group to use to successfully describe the structure of this perovskite as corroborated by reasonable bond lengths and the agreement factors as achieved by Rietveld refinement.

The Sr_2CoSbO_6 perovskite (air or O_2 synthesized) was described by Blasse (7) as cubic. However, as can be seen from Fig. 2 the (444) cubic reflection is split asymmetrically in intensity (compare to the former orthorhombic phase in Fig. 1), and a lower symmetry applies. The whole pattern can be indexed by assuming a monoclinic or rhombohedral unit cell. As the profile fits achieved for a monoclinic and a rhombohedral description were comparable, the higher symmetric structural model appeared to be appropriate.

[2] Lattice parameters have been normalized to the perovskite ideal cubic structure to allow for an easier comparison. The real structure is related to the cubic perovskite as follows: $a = \sqrt{2}a_p$, $b = \sqrt{2}a_p$, $c = 2a_p$.

The occupation factors obtained by refining the structure in the space group $R\bar{3}m$ (No. 166) indicate that the degree of ordering of B cations is not complete. About 77% of Co and 33% of Sb is in one B position and vice versa for the remaining one. This partial ordering could be explained mainly by the charge difference of 2 between the ions, although they present similar ionic radii (23) (Co^{3+} (HS) = 0.75, Co^{3+} (LS) = 0.685, Sb^{5+} = 0.74, in Å).

The ionic radius of Co^{3+} (either high or low spin) is smaller than that of Co^{2+} HS (0.885 Å) found in the former phase. Thus a decrease in the geometrical mismatch between the A–O and B–O bonds is to be expected ($t = 0.96$–0.97), and hence an increase in crystal symmetry. The lattice parameters obtained in the refinement are $a = 5.5992(2)$ Å and $c = 13.6609(2)$ Å. In the rhombohedral setting the following cell metric is obtained, $a = 5.5844$ Å and $\beta = 60.17^\circ$, and thus a strong cubic pseudosymmetry is evidenced by the small departure of the β angle from 60°.

The Ar-annealed sample shows an X-ray pattern that is fairly cubic (Fig. 3) and can be indexed in the $Fm\bar{3}m$ space group with a doubling of the lattice parameters with respect to the ideal cubic perovskite. The chemical analysis reveals a considerable oxygen deficiency ($Sr_2CoSbO_{5.63(1)}$) and hence the mean Co oxidation state is about + 2.25. In this case, since the Co^{2+} amount is higher, an increase in the geometrical mismatch between the A–O and B–O bonds should be expected and therefore a more distorted structure. But in this case as the perovskite is oxygen deficient, the octahedral tilting to minimize the mismatch is not so effective and moreover the rigidity of the BO_3 framework is lowered. This oxygen-defective perovskite must have disordered oxygen vacancies because in case of having ordered vacancies the high symmetry is not attained (superstructure reflections) and a tilting of the "octahedra" should be expected too. With regard to the B site, it is reasonable to find higher ordering at the B-site for the reduced perovskite, since the ionic radius of Co^{2+} is higher than that of Co^{3+} and Sb^{5+}, and moreover the charge difference is increased. The ratio as determined by Rietveld refinement (Table 2) is ca. 84% ordering vs 77% of the fully oxidized perovskite.

Magnetic Measurements

Figure 4 shows the molar magnetic susceptibility of $Sr_3CoSb_2O_9$ and its inverse as a function of the temperature as measured in an applied field of 0.1 T. An effective magnetic moment of 5.39 μ_B per Co^{2+} ion is obtained by fitting the magnetic data between 200 and 350 K to the Curie–Weiss law. This value is in the upper limit for Co^{2+} high spin in octahedral coordination with completely unquenched orbital contribution ($^4T_{1g}$ term), thus supporting that the CoO_6 octahedra are not strongly distorted. The negative value (− 96 K) of the Weiss parameter could be indicating that an antiferromagnetic long-range order of the

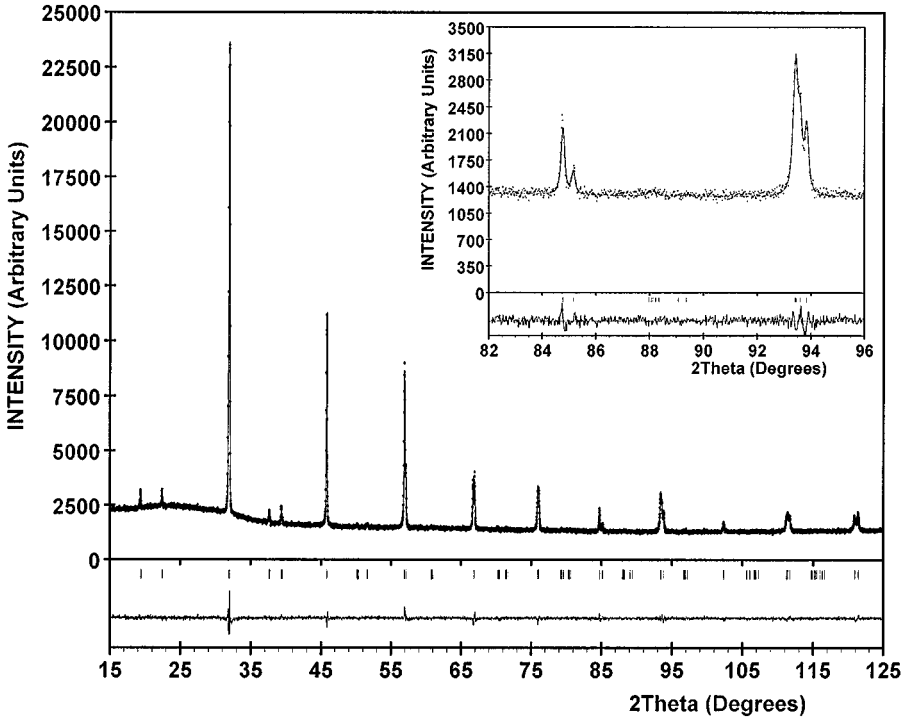

FIG. 2. Rietveld refinement profiles: observed (dots), calculated (solid line), difference (bottom solid line), and Bragg reflections (tick marks) for the fit to the Cu$K\alpha_1$ X-ray pattern of the Sr_2CoSbO_6 perovskite.

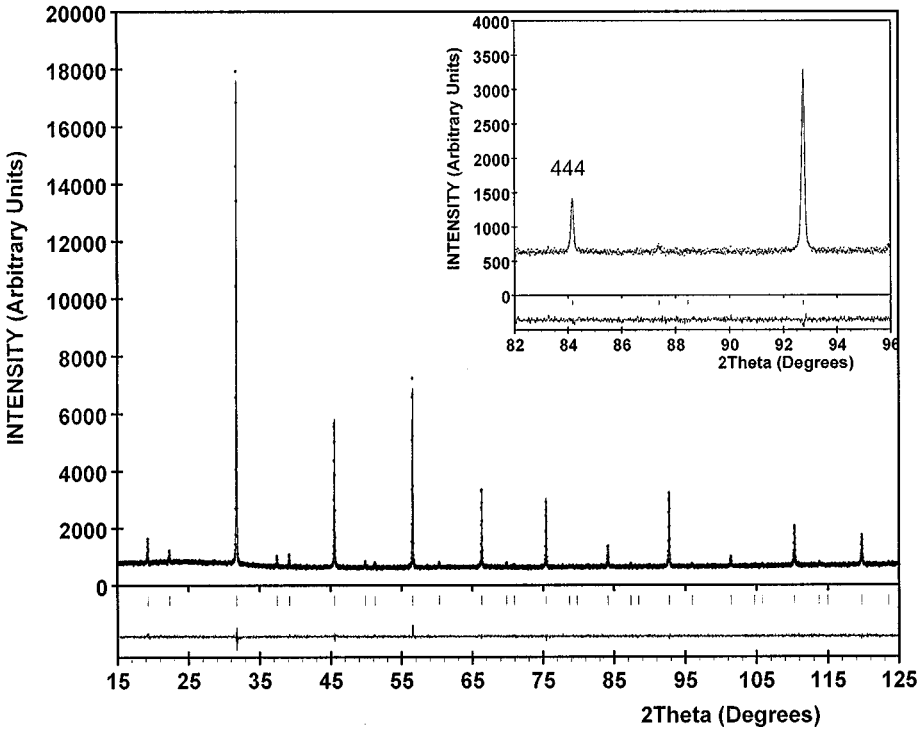

FIG. 3. Rietveld refinement profiles: observed (dots), calculated (solid line), difference (bottom solid line), and Bragg reflections (tick marks) for the fit to the Cu$K\alpha_1$ X-ray pattern of the $Sr_2CoSbO_{5.63}$ perovskite.

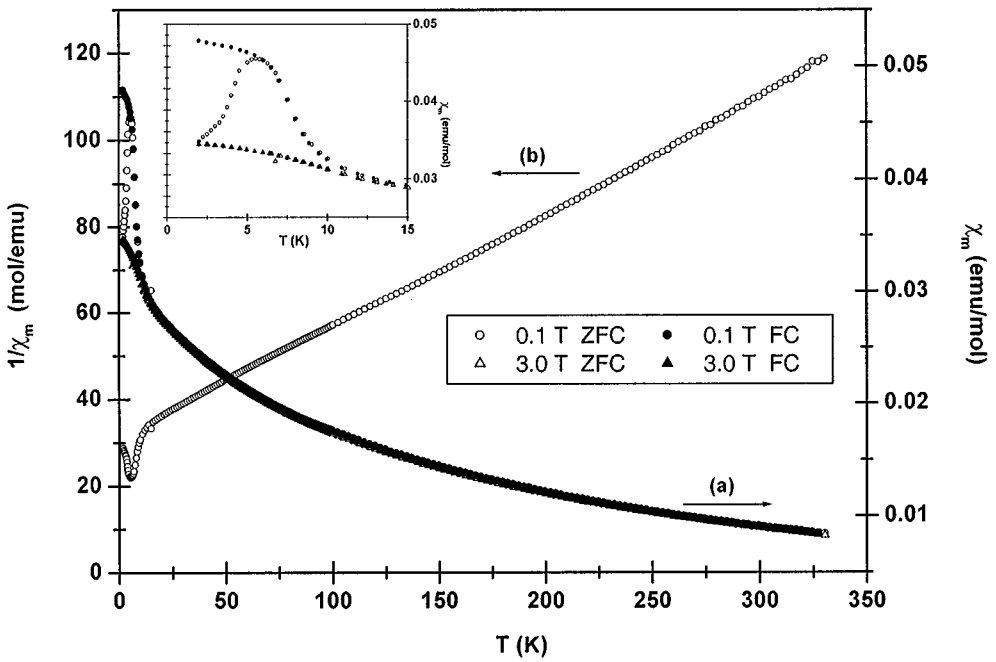

FIG. 4. The temperature dependence of (a) molar magnetic susceptibility χ_m and (b) the inverse of the molar magnetic susceptibility $1/\chi_m$ for $Sr_3CoSb_2O_9$ at 0.1 T (circle) and 3 T (triangle) in zero field cooling (open symbols) and field cooling (filled symbols).

Co^{2+} magnetic moments is established below a Neel temperature of ca. 6 K. But the difference between the curves of χ_m at 0.1 and 3 T below the temperature onset signals that more probably a spin-glass transition is taking place below that temperature with dominating antiferromagnetic coupling. The spin-glass state was supported by the irreversible behavior of the ZFC and FC measurements in low field (0.1 T) below the transition temperature (Fig. 4). Typical spin-glass transitions are due to the existence of different exchange interactions that are competing and hence giving rise to a certain degree of magnetic frustration (24). This is usually found in disordered structures and it has been particularly observed in $AB_xB'_{1-x}O_3$ perovskites when some degree of disorder at the B site is achieved for the magnetic ion (25). In $Sr_3CoSb_2O_9$ the Co^{2+} ions are almost completely located at one of the two B sites occupying 64%, and therefore they are disordered among 36% of diamagnetic Sb^{5+} ions that are at the same site. Moreover, as the ratio Sb^{5+}/Co^{2+} is 2, the system is magnetically diluted and the occurrence of the spin-glass transition at very low temperature is reasonable.

The variation of the molar susceptibility vs temperature for Sr_2CoSbO_6 has been measured at 0.1 T with ZCF and FC methods and is shown in Fig. 5 along with its inverse. In the temperature range between 150 and 700 K the compound reveals a Curie–Weiss behavior with $\mu_{eff} = 3.83$ μ_B and $\theta = -70$ K. This compound could be completely ordered in the B site since the appropriate stoichiometry condition is achieved (Sb/Co ratio is equal to 1), but from Rietveld refinement results (see Table 3) we deduced only 77% of ordering. This incomplete ordering at the B site along with a diluted magnetic system are the prerequisites necessary to obtain again a spin-glass transition at low temperatures as indicated by the departure of the χ_m data for ZFC and FC measurements at 0.1 T at temperatures below the onset, rather than an antiferromagnetic order with a $T_{Neel} \sim 47$ K as suggested by the maximum in the χ_m curve and the negative sign of the Curie–Weiss parameter. In this compound the spin-glass transition takes place at a higher temperature, due to several factors: it is less magnetically diluted due to the higher Co/Sb ratio, and the magnetic ion is different (Co^{2+} vs Co^{3+}) hence the strength and nature of the exchange interactions are different.

Depending upon the strength of the crystal field Co^{3+} can be present in a high- or low-spin state in octahedral coordination. The HS state $t_{2g}^4 e_g^2$ is achieved in weak octahedral ligand fields and is a $^5T_{2g}(^5D)$ term that gives rise to an important orbital contribution to the magnetic moment. The LS state (t_{2g}^6) occurs in strong fields and has a $^1A_{1g}(^1I)$ term. In addition an intermediate spin (IS) state ($t_{2g}^5 e_g^1$), $^3T_{1g}(^3H)$ term, is found that is a low-lying excited state when close to the crossover point. HS Co^{3+} in an octahedral ligand field is usually found in complex fluorides only. The IS state can be the ground state in lower symmetries like axially distorted octahedra (26). The effective magnetic moment determined $\mu_{eff} = 3.83$ μ_B is in between the magnetic moment for a HS state with spin only contribution ($S = 2$, 4.9 μ_B) and a IS state ($S = 1$, 2.8 μ_B). But this is

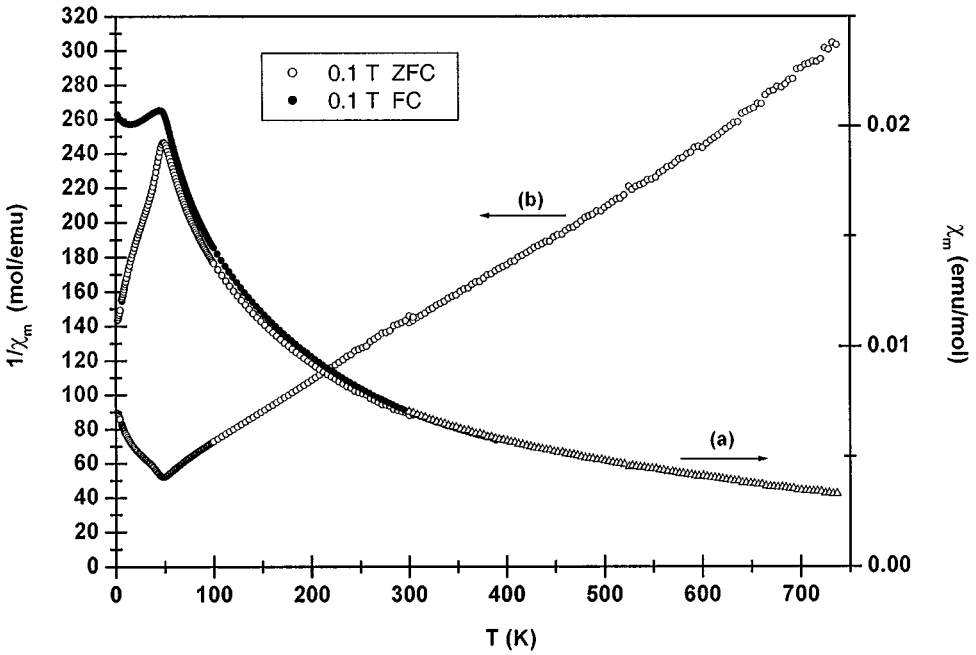

FIG. 5. Temperature dependence of (a) the molar magnetic susceptibility χ_m and (b) the inverse of the molar magnetic susceptibility $1/\chi_m$ for Sr_2CoSbO_6 at 0.1 T in zero field cooling (open symbols) and field cooling (filled symbols).

contradictory to the conclusions stated by Blasse who found an effective magnetic moment of 5.2 μ_B per cobalt ion (8), which is higher than the predicted by spin only value (4.9 μ_B), and thus he considered that this perovskite was in a completely HS state. In the air synthesized sample that is slightly oxygen deficient, $Sr_2CoSbO_{5.95}$, the calculated effective magnetic moment is 4.35 μ_B and thus this increase should be ascribed to the formation of Co^{2+} ions. Therefore a similar effect could be the explanation why in Blasse's sample a higher μ_{eff} was obtained, because he did not use any high oxygen pressure method for synthesizing the perovskites.

The magnitude of the ligand field (Δ_{oct} in 6) depends on several parameters, the most important one being the overlap between the atomic orbitals of cobalt and oxygen yielding σ- and π-type interactions. Tuning the anion electronegativity is possible by changing its chemical environment. In this case, the electronegativity of oxygen is directly influenced by its respective cation surrounding, which can either be OSr_4Sb_2 or OSr_4CoSb. Of course, the polarization of oxygen by Sb^{5+} is stronger than that by Co^{3+}, and it is much more effective on the atomic orbitals that produce the σ interaction than on those that produce the π interaction. Hence a decrease in crystal field splitting is to be expected with increasing counter polarization of oxygen. On the other hand the π-type interaction is significantly influenced by the overlap between the O p_π orbitals and the t_{2g} orbitals of the cation; thus, a tilting of the octahedra will change the M–O–M 180° angle and a reduction in the π overlapping (decrease of Δ_π) will give rise to an increase in the Δ_{oct} (see Fig. 6) favoring the LS state. In this compound only a very slight departure from 180° is to be expected because of the very small distorted structure and, therefore, promoting the HS state. Therefore a change from LS to HS could be achieved by varying the chemical environment around the anions, due to modification of the oxygen electronegativity and the octahedra tilting (t factor analysis).

TABLE 2
Results of the X-Ray Refinement of $Sr_2CoSbO_{5.63}$ in the Space Group $Fm\bar{3}m$ (No. 225)

Atom	Site	x	y	z	B_{iso} (Å^2)	Occupancy
Sr	8c	0.25	0.25	0.25	0.98(6)	1
Co(1)	4a	0	0	0	0.17(11)	0.836(6)
Sb(1)						0.164(6)
Co(2)	4b	0.5	0.5	0.5	0.28(6)	0.164(6)
Sb(2)						0.836(6)
O	24e	0.2536(13)	0	0	2.47(16)	0.938

Note. Lattice parameters (Å): $a = 7.9658(1)$, R factors(%): $R_{wp} = 3.6$, $R_p = 2.9$, $R_F = 4.75$, $\chi^2 = 1.0$.

$YCoO_3$ and $LaCoO_3$ constitute a good example to compare how the effect of the lattice distortion (by means of octahedral tilting) and the change in the oxygen electronegativity, commented above, govern the crystal field splitting (27). Since the ionic radius of Y^{+3} is smaller than

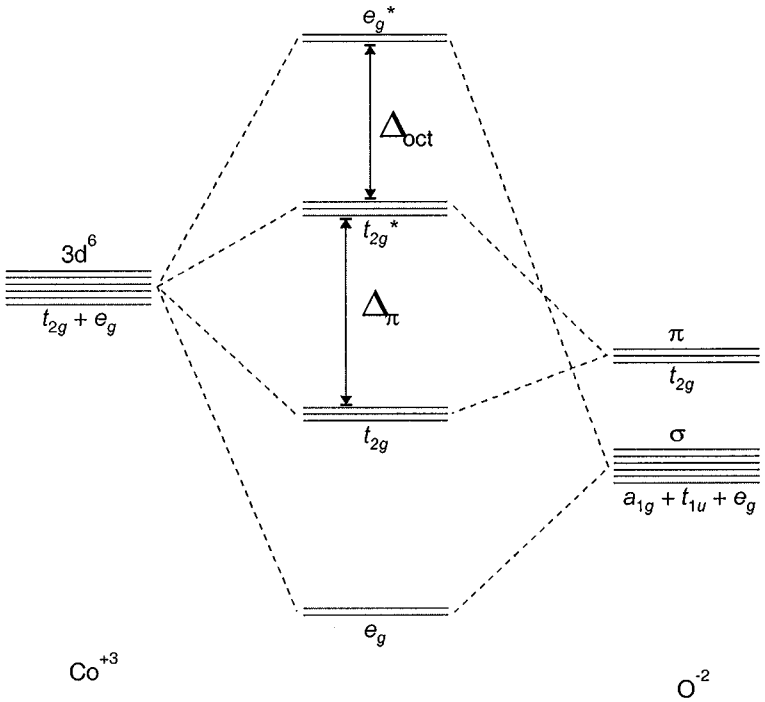

FIG. 6. *M*O diagram of octahedral Co^{+3}–O^{-2} σ- and π-type interactions showing the ligand-field splitting magnitude (Δ_{oct}). The larger is the departure of the *M*–O–*M* bond from 180° the smaller is Δ_π and therefore the greater is Δ_{oct}.

that of La^{3+} an enhancement of the oxygen electronegativity should be expected and hence a decrease of the crystal field splitting. But as the orthorhombic structure of $YCoO_3$ is much more distorted, the π orbital overlapping is weaker (smaller Δ_π) and therefore an increase of Δ_{oct} is attained as demonstrated by its higher spin transition temperature (ca. 420 K vs 110 K, respectively). In the case of Sr_2CoSbO_6, the oxygen electronegativity is significantly enhanced by the high polarizing power of the cation Sb^{5+}, and moreover the structure is not so distorted compared to that of $YCoO_3$. Thus both effects are in the same direction and therefore Δ_{oct} is expected to be even lower than in $LaCoO_3$.

A low-ligand field splitting for Sr_2CoSbO_6 is in agreement with the susceptibility results that show no LS state at low temperatures and a $\mu_{eff} = 3.83\ \mu_B$ constant in a very wide temperature range. This value is in between (ca. 50%) the magnetic moment for a HS state with spin only contribution ($S = 2$, 4.9 μ_B) and an IS state ($S = 1$, 2.8 μ_B). Some scenarios could account for such an *intermediate* magnetic moment, the following being the most plausible ones: (1) the stabilization of Co^{3+} ions in *IS* state (along with HS Co^{3+}) by means of an elongated octahedral coordination either by dynamic or static arrangement of the oxygens around the Co^{3+} ions (Jahn–Teller distortions) or (2) just by presenting the same features as Sr_2FeNbO_6 (28), in which the Fe^{3+} ions are in HS state but an effective magnetic moment lower than expected is calculated because it is a completely disordered perovskite exhibiting a spin-glass transition (ca. 33 K). In such situations where there exists a nonperfect spin randomness within the clusters and an antiferromagnetic spin correlation dominates, a μ_{eff} lower than the paramagnetic single one is obtained.

In conclusion, it can be stated clearly that no pure LS state is attained even at lower temperatures in Sr_2CoSbO_6, contrary to $LaCoO_3$ and $YCoO_3$, among others. Further experiments using neutron diffraction are in progress to determine unambiguously the oxygen substructure and hence to describe the best *scenario* for explaining the magnetic properties observed in this Co^{3+} perovskite.

Magnetic susceptibility measurements for the Ar-annealed sample, $Sr_2CoSbO_{5.63}$, at ZFC and FC applying different fields (0.1 and 3T) are shown in Fig. 7. A Curie–Weiss law is obeyed in the temperature range 75–300 K with an effective paramagnetic moment $\mu_{eff} = 4.85\ \mu_B$ per ion and a Weiss temperature $\theta = -136$ K, which indicates that dominant antiferromagnetic interactions exist among the cobalt ions (ca. 25% Co^{3+} and 75% Co^{2+}). The existence of an irreversible behavior as reflected by the ZFC and FC data below the onset temperature at 0.1 T signals that a transition from a paramagnetic to a spin-glass state occurs in this perovskite at ca. 14 K. Although this compound was determined to be more ordered compared to the full oxygen stoichiometric perovskite, an additional source of disorder results due to the presence of a further magnetic ion, Co^{2+}. Thus, to expect a similar spin-glass behavior is reasonable.

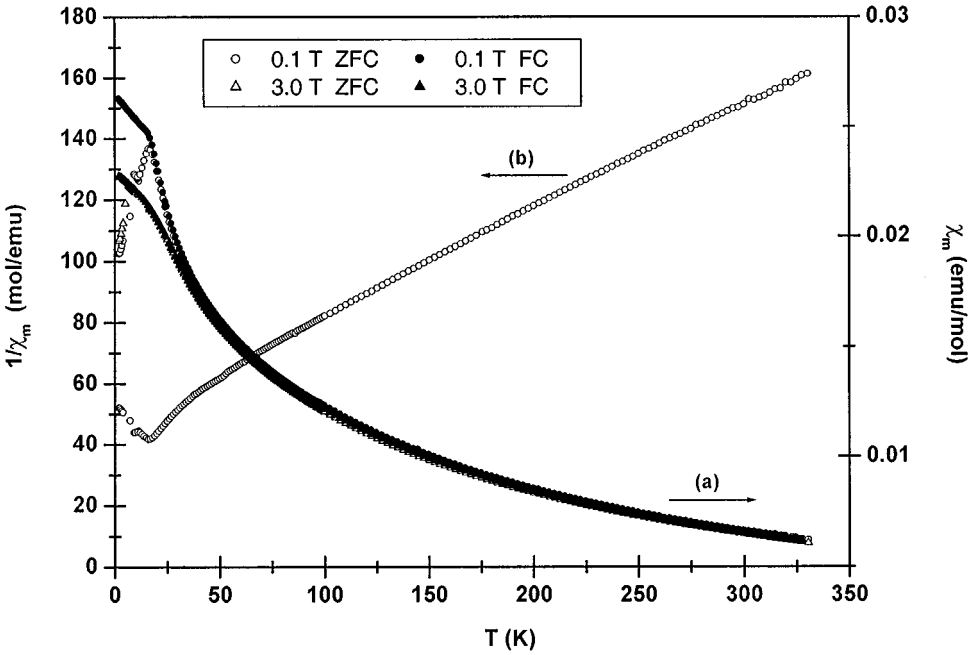

FIG. 7. Temperature dependence of (a) the molar magnetic susceptibility χ_m and (b) the inverse of the molar magnetic susceptibility $1/\chi_m$ for $Sr_2CoSbO_{5.63}$ at 0.1 T (circle) and 3 T (triangle) in zero field cooling (open symbols) and field cooling (filled symbols).

Electrical Measurements

Resistivity (ρ) measurements were carried out on polycrystalline sintered pellets between 300 and 4 K. $Sr_3CoSb_2O_9$ revealed an insulator behavior, while Sr_2CoSbO_6 and $Sr_2CoSbO_{5.63}$ presented semiconductor properties with room temperature resistivities of ca. 3 k$\Omega\cdot$cm and 70 k$\Omega\cdot$cm, respectively. An estimation of the $Sr_2CoSbO_{5.63}$ band gap was performed by fitting the resistivity data to the Mott variable-range hopping equation $\rho = \rho_0 \exp((T_0/T)^p)$ (29). The experimental data fit reasonably well ($R = 0.9989$ and 0.9992 for $p = \frac{1}{3}$ and $p = \frac{1}{4}$, respectively) either to the bidimensional ($p = \frac{1}{3}$) or the three-dimensional ($p = \frac{1}{4}$) hopping model; thus for both cases an activation energy of 0.27(1) eV in the temperature range 150–300 K was calculated. This ambiguity in determining the dimensionality of the hopping model could be attributed to the partial disorder observed in *B* cations and/or in oxygen positions.

TABLE 3
Results of the X-Ray Refinement of Sr_2CoSbO_6 in the Space Group $R\bar{3}m$ (No. 166)

Atom	Site	*x*	*y*	*z*	B_{iso} (Å^2)	Occupancy
Sr	4i	0	0	0.2505(4)	0.88(7)	1
Co(1)	2d	0	0	0.5	0.86(14)	0.228(6)
Sb(1)						0.772(6)
Co(2)	2a	0	0	0	0.21(8)	0.772(6)
Sb(2)						0.228(6)
O	4i	0.1653(14)	−0.1653(14)	0.5818(11)	2.09(12)	1

Note. Lattice parameters (Å): $a = 5.5992(2)$, $c = 13.6609(2)$, *R* factors (%): $R_{wp} = 3.01$, $R_p = 2.39$, $R_F = 7.19$, $\chi^2 = 1.47$.

ACKNOWLEDGMENTS

We thank O. Buresch for the ICP-OES measurements, E. Bruecher and R. Kremer for the susceptibility measurements, G. Siegle for the resistivity measurements, and P. Kazin and P. Adler for helpful discussions and critical review of the manuscript.

REFERENCES

1. Y. Minet, V. Lefranc, N. Nguyen, B. Domengès, A. Maignan, and B. Raveau, *J. Solid State Chem.* **121,** 158 (1996).
2. S. Kawsaki, M. Takano, and Y. Takeda, *J. Solid State Chem.* **121,** 174 (1996).
3. A. Lappas, K. Prassides, F. N. Gygax, and A. Schenk, *J. Solid State Chem.* **145,** 587 (1999).
4. A. Maignan, C. Martin, D. Pelloquin, N. Nguyen, and B. Raveau, *J. Solid State Chem.* **142,** 247 (1999).
5. M. Itoh, I. Natori, I. Kubota, and K. Motoya, *J. Phys. Soc. Jpn.* **63,** 1486 (1994).
6. S. H. Kim and P.D. Battle, *J. Solid State Chem.* **114,** 174 (1995).
7. G. Blasse, *J. Inorg. Nucl. Chem.* **27,** 993 (1965).
8. G. Blasse, *J. Appl. Phys.* **36,** 879 (1965).
9. I. G. Main, J. F. Marshall, G. Demazeau, G. A. Robins, and C. E. Jonhson, *J. Phys. C: Solid State Phys.* **12,** 2215 (1979).
10. (a) M. A. Señarís-Rodríguez and J. B. Goodenough, *J. Solid State Chem.* **116,** 224 (1995); (b) J. B. Goodenough and J.-S. Zhou, *Chem. Mater.* **10,** 2980 (1998).

11. K. Asai, A. Yoneda, O. Yokokura, J. M. Tranquada, G. Shirane, and K. Hohn, *J. Phys. Soc. Jpn.* **67,** 290 (1998); M. Itoh, M. Mori, S. Yamaguhi, and Y. Tokura, *Phys. B* **259–261,** 902 (1999).
12. K. Yoshii, *J. Solid State Chem.* **151,** 294 (2000).
13. J. P. Doumerc, J. C. Grenier, P. Hagenmuller, M. Pouchard, and A. Villesuzanne, *J. Solid State Chem.* **147,** 211 (1999).
14. N. Ichinose, Y. Ozaki, and S. Kashu, "Superfine Particles Technology," Chap. 5. Springer-Verlag, Berlin, 1992.
15. J. Rodriguez-Carvajal, *Physica B* **192,** 55 (1993).
16. V. Primo-Martín, *Powder Diffract.* **14,** 70 (1999).
17. P. W. Selwood, "Magnetochemistry." Interscience, New York, 1943.
18. R. L. Carlin, "Magnetochemistry," p. 12. Springer-Verlag, Berlin/Heidelberg, 1986.
19. S. F. A. Kettle, "Physical Inorganic Chemistry," p. 191. Spectrum Academic Publishers, 1996.
20. G. Demazeau, *Eur. J. Sol. State Inorg.* **34,** 759 (1997).
21. A. M. Glazer, *Acta Crystallogr. A* **31,** 756 (1975).
22. P. M. Woodward, *Acta Crystallogr. B* **53,** 44 (1997).
23. R. D. Shannon, *Acta Crystallogr. A* **32,** 751 (1976).
24. K. Moorjani and J. M. D. Coey, "Magnetic Glasses," p. 36. Elsevier, Amsterdam, 1984.
25. P. D. Battle, T. C. Gibb, C. W. Jones, and F. Studer, *J. Solid State Chem.* **78,** 281 (1989).
26. B. Buffat, G. Demazeau, M. Pouchard, and P. Hagenmuller, *Proc. Indian Acad. Sci.* **93,** 313 (1984).
27. G. Demazeau, M. Pouchard, and P. Hagenmuller, *J. Solid State Chem.* **9,** 202 (1974).
28. R. Rodríguez, A. Fernández, A. Isalgué, J. Rodríguez, A. Labarta, J. Tejada, and X. Obradors, *J. Phys. C: Solid State Phys.* **18,** L401 (1985).
29. B. Fisher, G. Koren, J. Genossar, L. Patlagem, and E. L. Gartstein, *Physica C* **176,** 75 (1991).